

The physical relation between disc and coronal emission in quasars

Lusso Elisabeta^{1,*} and Risaliti Guido^{2,3}

¹Centre for Extragalactic Astronomy, Durham University, South Road, Durham, DH1 3LE, UK

²Dipartimento di Fisica e Astronomia, Università di Firenze, via G. Sansone 1, 50019 Sesto Fiorentino, Firenze, Italy

³INAF–Osservatorio Astrofisico di Arcetri, 50125 Florence, Italy

Correspondence*:
Corresponding Author
elisabeta.lusso@durham.ac.uk

ABSTRACT

We propose a modified version of the observed non-linear relation between the X-ray (2 keV) and the ultraviolet (2500 Å) emission in quasars (i.e. $L_X \propto L_{UV}^\gamma$) which involves the full width at half-maximum, $FWHM$, of the broad emission line, i.e. $L_X \propto L_{UV}^\gamma FWHM^\beta$. By analysing a sample of 550 optically selected non-jetted quasars in the redshift range of 0.36–2.23 from the Sloan Digital Sky Survey cross matched with the XMM-Newton catalogue 3XMM-DR6, we found that the additional dependence of the observed $L_X - L_{UV}$ correlation on the $FWHM$ of the MgII broad emission line is statistically significant. Our statistical analysis leads to a much tighter relation with respect to the one neglecting $FWHM$, and it does not evolve with redshift. We interpret this new relation within an accretion disc corona scenario where reconnection and magnetic loops above the accretion disc can account for the production of the primary X-ray radiation. For a broad line region size depending on the disc luminosity as $R_{blr} \propto L_{disc}^{0.5}$, we find that $L_X \propto L_{UV}^{4/7} FWHM^{4/7}$, which is in very good agreement with the observed correlation.

Keywords: active galactic nuclei, quasar, supermassive black holes, accretion disc, X-ray

1 INTRODUCTION

One of the observational evidences for the link between the accretion disc and the X-ray corona in active galactic nuclei (AGN) is given by the observed non-linear correlation between the monochromatic ultraviolet luminosity at 2500 Å (L_{UV}) and the one in the X-rays at 2 keV (L_X). Such relationship (parameterised as $\log L_X = \gamma \log L_{UV} + \beta$) exhibits a slope, γ , around 0.6, implying that optically bright AGN emit relatively less X-rays than optically faint AGN [1]. The value of the slope in this relation does not depend on the sample selection, the correlation is also very tight (~ 0.24 dex, Lusso and Risaliti 2), and independent on redshift [3, 4, 5, 6, 7, 8, 9, 10, 11]. Recently, the $L_X - L_{UV}$ relationship (or, more precisely, its version with fluxes) has also been employed as a distance indicator to estimate cosmological parameters such as Ω_M and Ω_Λ by building a Hubble diagram in a similar way as for Type Ia supernovae [12, 13, and references therein], but extending it up to $z \sim 6$ [14, 15]. Yet, the challenge in interpreting such relation on physical grounds is that the origin of the X-ray emission in quasars is still a matter of debate.

Some attempts at explaining the quasar X-ray spectra were based upon the reprocessing of radiation from a non-thermal electron-positron pair cascade (e.g. Svensson 16, 17, Zdziarski et al. 18). Another

possibility rests on a two-phase accretion disc model, where a fraction f of gravitational power is dissipated via buoyancy and reconnection of magnetic fields in a uniform, hot ($T_{\text{cor}} \sim 100 \text{ keV} \sim 10^9 \text{ K}$) plasma close to the cold opaque disc [19, 20, 21, 22, 23]. The scenario for this model is the following. Phase 1 is the optically thick “cold” (tens of eV) disc, whilst phase 2 is a hot optically thin plasma located above (and below) the disc. The seed disc photons illuminate the hot tenuous plasma, and a fraction of them is up-scattered to hard X-rays via inverse Compton scattering, providing the main source of cooling of the plasma. About half of these hard X-ray photons is irradiated back to the disc, contributing to its energy balance, whilst the rest escape and are observed. A stable disc-corona system is then in place only if there is a strong coupling between ultraviolet and X-ray photons. This model retrieves the photon index slope of the coronal X-ray spectrum (i.e. $\Gamma_X \simeq 2$), in close agreement with real data. Nonetheless, it also predicts a nearly equal amount of ultraviolet and X-ray radiation (i.e. $\gamma = 1$), which is not in agreement with the observed correlation. If the corona is not uniform, but a rather patchy medium, and only a fraction (f) of the accretion power is released in the hot phase, the resulting γ value is < 1 , but one needs to consider a rather arbitrary number of active blobs [24]. Magnetic field turbulence has been recognised not only as an additional heating mechanism in the formation of the corona (e.g. Galeev et al. 25, Merloni and Fabian 26, Liu et al. 27), but also as an efficient means for the transport of the disc angular momentum (e.g. Balbus 28). Yet, the value of the fraction f of gravitational power dissipated in the hot corona (needed for keeping the plasma at high temperatures), and how the coronal physical state depends on the black hole mass and disc accretion rate still remain a matter of debate.

In Lusso and Risaliti [29] we outlined a simple but physically motivated, ad-hoc model to interpret the observed correlation between the ultraviolet and the X-ray emission in terms of physical parameters such as the black hole mass (M_{BH} , here we considered the normalized value $m = M_{\text{BH}}/M_{\odot}$), the accretion rate ($\dot{m} = \dot{M}/\dot{M}_{\text{Edd}}$, where \dot{M}_{Edd} is the accretion rate at Eddington), and the distance to the black hole ($r = R/R_S$, where $R_S = 2GM_{\text{BH}}/c^2$ is the Schwarzschild radius). Our main aim was to link such relations with observable quantities (i.e. the observed ultraviolet and X-ray luminosities), thus obtaining a relation that can be then compared with the data.

Here, we further analyse the $L_X - L_{\text{UV}} - FWHM$ relation with the goal of understanding its physical origin in the context of black hole accretion physics.

2 THE OBSERVED $L_X - L_{\text{UV}} - FWHM$ PLANE

The quasar sample considered by Lusso and Risaliti [29] is obtained by cross-matching the quasar SDSS catalogue published by Shen et al. [30] with the serendipitous X-ray source catalogue 3XMM-DR6 [31]. Filters are also applied in order to select a clean quasar sample where biases and contaminants are minimised, namely: (i) jetted, broad absorption line quasars and sources with high levels of absorption in the optical ($E(B - V) > 0.1$) are removed from the sample; (ii) we selected those quasars with a full-width half-maximum, $FWHM$, for the MgII $\lambda 2800 \text{ \AA}$ higher than 2000 km s^{-1} ; (iii) only sources with good X-ray data (i.e. $S/N > 5$ in the 0.2–12 keV EPIC band) and low levels of X-ray absorption (i.e. with an X-ray photon index $\Gamma_X > 1.6$) are considered; and finally (iii) the *Eddington bias* (see also Risaliti and Lusso 14 and Lusso and Risaliti 2 for further details) is minimised by including only quasars whose minimum detectable X-ray flux is lower than the expected one in each observation. The $FWHM$ values for the MgII emission line as well as the ultraviolet 2500 \AA luminosities are taken from the Shen et al. [30] catalogue, which have been measured from the continuum/emission line fitting of the SDSS spectra (see their Section 3 for further details). The final clean sample is composed of 550 quasars and it is only $\sim 25\%$ of the initial sample ($\sim 2,100$ quasars with both soft 0.5–2 keV and hard 2–12 keV fluxes),

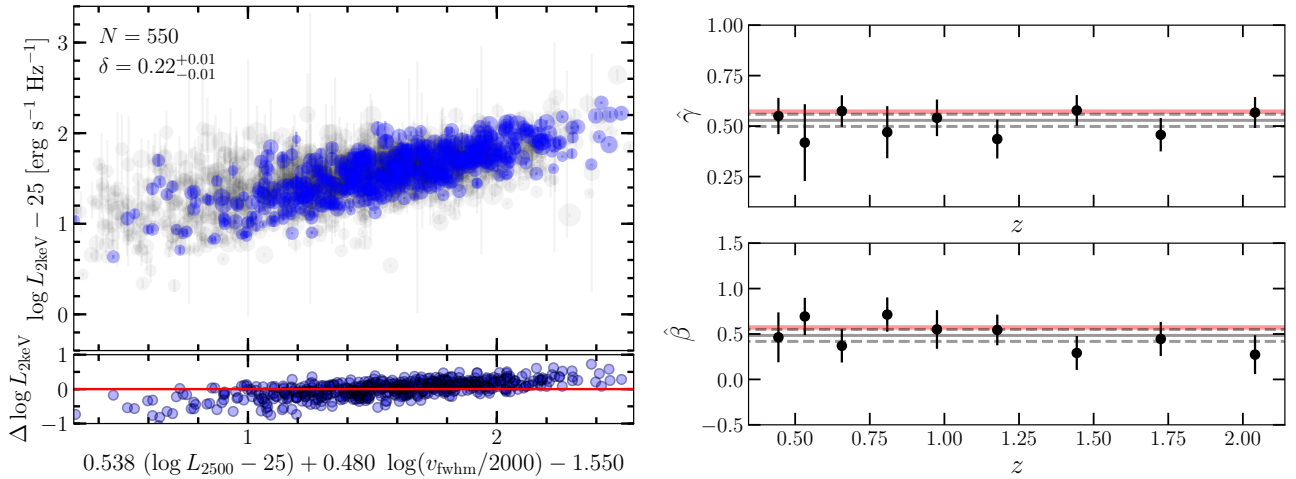


Figure 1. Left: The tight $L_X - L_{UV} - FWHM$ plane (seen edge-on) for the $z < 2.3$ SDSS-3XMM-DR6 quasar sample in Lusso & Risaliti (2017). The full-width half maximum ($FWHM$) is computed from the MgII emission line. The size of the points has been rescaled to the $FWHM$ value, the smaller size corresponds to $FWHM = 2000$ km/s. The slopes of this correlation are in very good agreement (within the uncertainties) with the ones predicted by our simple (but physically motivated) model, $L_X \propto L_{UV}^{\hat{\gamma}} FWHM^{\hat{\beta}}$, where $\hat{\gamma} = \hat{\beta} = 4/7$ ($4/7 \sim 0.571$). The quasar sample before applying our filters is also plotted with light grey points. Right: Slopes of the $L_X - L_{UV} - FWHM$ plane as a function of redshift. The red solid line represents the predicted value of $4/7$. The observed $L_X - L_{UV} - FWHM$ plane does not evolve with redshift up to $z \sim 2.3$, which is an essential requirement in order to utilize this relation to measure cosmological parameters. The grey solid and dashed lines represent the weighted means and uncertainties of the black points, respectively. Figure based on data derived from Lusso & Risaliti (2017).

resulting from the stringent filters mentioned above. In the future we will refine the treatment of the systematics by considering additional instrumental systematics, and developing large mock simulations to better understand the impact of the Eddington bias on the results. The main aim is to reduce the rejection fraction, thus maximizing the statistics of the final sample.

Figure 1 shows an edge-on view of the $L_X - L_{UV} - FWHM$ plane. The best-fit regression relation for this quasar sample is

$$(\log L_X - 25) = (0.538 \pm 0.022)(\log L_{UV} - 25) + (0.480 \pm 0.078)[\log FWHM - (3 + \log 2)] + (-1.550 \pm 0.122), \quad (1)$$

with an observed dispersion of 0.22 dex, which is a very tight relation. To fit the data, we adopted *emcee* [32], which is a pure-Python implementation of Goodman & Weare’s affine invariant Markov chain Monte Carlo ensemble sampler.

We then divided the quasar sample into equally spaced narrow redshift intervals in $\log z$ with a $\Delta \log z < 0.1$ to minimise the scatter due to the different luminosity distances within each interval. We split the sample into 10 intervals with $\Delta \log z = 0.08$ and, for each redshift interval, we performed a fit of the $F_X - F_{UV} - FWHM$ relation, $\log F_X = \hat{\gamma}_z \log F_{UV} + \hat{\beta}_z FWHM + \hat{K}$, with free $\hat{\gamma}_z$ and $\hat{\beta}_z$. The results for the best-fit slopes $\hat{\gamma}_z$ and $\hat{\beta}_z$ as a function redshift are shown in Figure 1. Despite the large scatter, both $\hat{\gamma}_z$ and $\hat{\beta}_z$ slopes do not show any significant evolution with time and they are consistent with a constant value in the redshift interval 0.3–2.

3 THE TOY MODEL

Previous works in the literature suggest that the amount of gravitational energy from the accretion disc released in the hot plasma surrounding the disc itself, likely depends on the black hole mass M_{BH} , the mass accretion rate \dot{M} , and the spin of the black hole. In Lusso and Risaliti [29], the $L_X - L_{\text{UV}}$ correlation was reproduced if the energy transfer from an optically thick, geometrically thin accretion disc to the corona is confined to the gas-pressure dominated region of the disc. In such simple model, the monochromatic ultraviolet and X-ray luminosities show an extra dependence on the $FWHM$, thus on the black hole mass and accretion rate as $L_{\text{UV}} \propto M_{\text{BH}}^{4/3} (\dot{M}/\dot{M}_{\text{Edd}})^{2/3}$ and $L_X \propto M_{\text{BH}}^{19/21} (\dot{M}/\dot{M}_{\text{Edd}})^{5/21}$, respectively. Assuming a broad line region size function of the disc luminosity as $R_{\text{blr}} \propto L_{\text{disc}}^{0.5}$ we have that

$$L_X \simeq 6 \times 10^4 L_{\text{UV}}^{4/7} FWHM^{4/7} \alpha^{-2/21} \kappa^{2/7} \times (1-f)^{-6/7} J(r)^{-16/21} \text{ erg s}^{-1} \text{ Hz}^{-1}, \quad (2)$$

where α is the standard disc viscosity parameter, κ is a calibration constant in the broad line region radius-luminosity relation (i.e. $R_{\text{blr}} = \kappa L_{\text{bol}}^{0.5}$ Trippe 33), and $J(r) = (1 - \sqrt{3/r})$.

In this model the bulk of the radiation budget of the X-ray corona is measured at the transition radius (r_{tr}) where the gas pressure in the accretion disc equates the radiation pressure, and it is defined as

$$r_{\text{tr}} \simeq 120 (\alpha m)^{2/21} \dot{m}^{16/21} (1-f)^{6/7} J(r)^{16/21}, \quad (3)$$

where $m = \frac{M_{\text{BH}}}{M_{\odot}}$, and $\dot{m} = \frac{\dot{M}}{\dot{M}_{\text{Edd}}}$. The transition radius can vary from a few gravitational radii (r_g) to several hundreds r_g for a black hole mass $m = 10^{8-9}$, with an accretion rate in the range $\dot{m} = 0.1 - 0.3$, and $\alpha = 0.4$. This parameter also depends on the value of f (i.e. the higher is f , the smaller is r_{tr}). Yet, the effective location of the corona may also be placed at small radii of less than tens of r_g . From a qualitative perspective, the torque (caused by the disc rotation) of magnetic field lines (originated at $r \geq r_{\text{tr}}$) that connects two opposite sides of the accretion disc (e.g. *magnetic reconnection*, a schematic representation of our model is provided in Figure 2) could cause particle acceleration at the magnetic reconnection site, located closer to the black hole (at $r < r_{\text{tr}}$), where particles lose their energy radiatively via the inverse Compton process.

4 CONSTRAINING THE FRACTION OF ACCRETION POWER RELEASED IN THE CORONA

Our simple (but physically motivated) model also provides constraints on the fraction of accretion power released in the hot plasma in the vicinity of the accretion disc, f , as a function of the broad line region size, from the observed normalization of $L_X - L_{\text{UV}} - FWHM$ plane.

Figure 3 shows how the normalization of equation (2) changes as a function of α , κ , and f . We fixed the κ factor to 1.3×10^{-6} , which corresponds to a broad line region size of about 1.3×10^{17} cm (~ 50 light days) and a bolometric luminosity of 10^{46} erg s $^{-1}$, typical of quasars (e.g. Kaspi et al. 34). The viscosity parameter varies from 0.1 to 0.4 [35], whilst f ranges in the interval 0–0.99. Although the normalization of the relation displays a large scatter, which can be a factor of ~ 2 in logarithm (i.e. orders of magnitude), the data suggest a value of f in the range 0.9–0.95.

In the future, by studying larger sample of quasars with M_{BH} and accretion rate values (which are all related to f), we will compare our results on f with the expectations from numerical simulations (e.g. Jiang et al. 36) and other theoretical models (e.g. Merloni and Fabian 26, Cao 37, Liu et al. 38), especially those

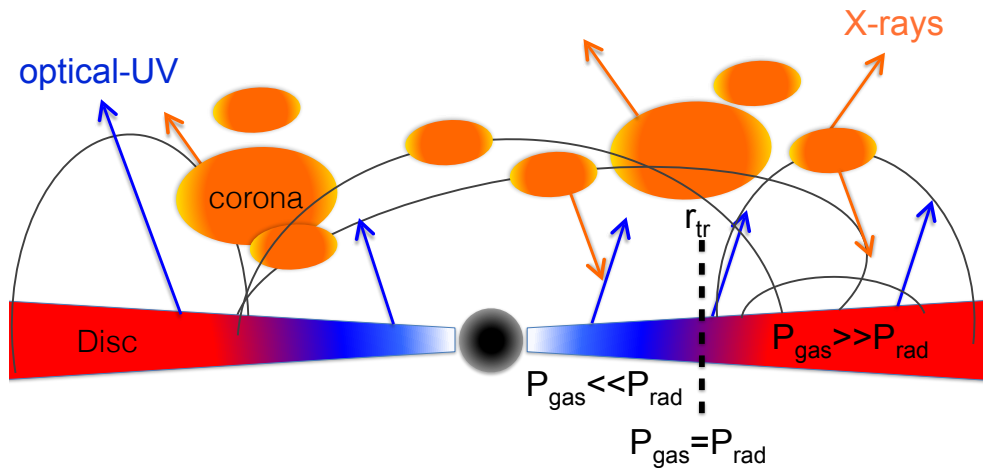


Figure 2. A schematic representation of the toy model discussed in §3. The optically thick, geometrically thin accretion disc emits the seeds photons that illuminate the hot tenuous (possibly clumpy) plasma. A fraction of them is up-scattered to hard X-rays via inverse Compton scattering. Part of these hard X-ray photons is irradiated back to the disc, contributing to its energy balance, whilst the rest escape and are observed. Stable magnetic loop can be formed only in the radiation pressure dominated part of the disc.

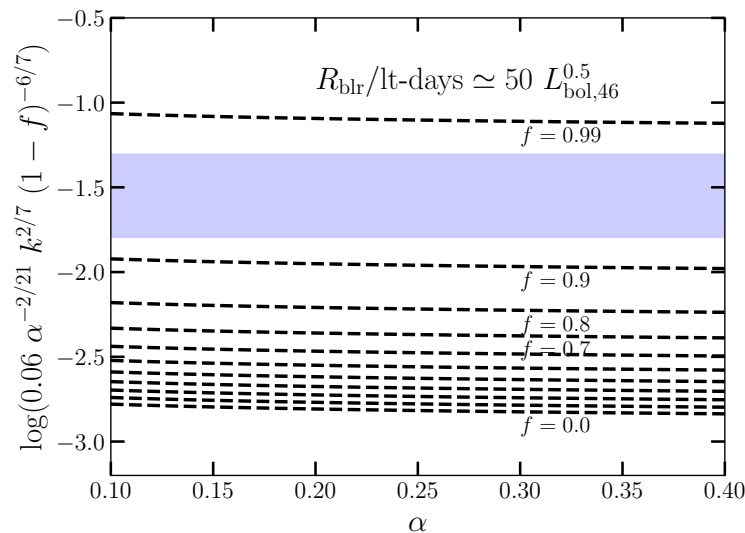


Figure 3. The logarithm of the normalization of equation (2) as a function of the accretion disc viscosity, α . The factor κ is fixed to 1.3×10^{-6} , which corresponds to a broad line region size of about 1.3×10^{17} cm (~ 50 light days) and $L_{\text{bol}} = 10^{46}$ erg s $^{-1}$. The dashed black lines represent different values of f in the range from 0 to 0.99. The blue shaded area indicates the observed range of the normalization of the $L_X - L_{\text{UV}} - FWHM$ plane in a sample of ~ 500 quasars. Figure based on data derived from Lusso & Risaliti (2017).

concerning the physical state and extent of the broad line region (e.g. Failed Radiatively Accelerated Dusty Outflows, FRADO, Czerny et al. 39).

5 CONCLUSIONS

Our modified $L_X - L_{\text{UV}}$ relationship in quasars, which takes into account the full-width half-maximum of the quasar emission line (i.e. $L_X \propto L_{\text{UV}}^{\hat{\gamma}} FWHM^{\hat{\beta}}$), has an observed dispersion of ~ 0.2 dex over ~ 3 orders

of magnitude in luminosity and indicates that there is a good “coupling” between the disc, emitting the primary radiation, and the hot-electron *corona*, emitting X-rays.

We interpreted such relation through a simple (but physically motivated) model based on the ones presented by Svensson and Zdziarski [21] and Merloni and Fabian [26], where a geometrically thin, optically thick accretion disc is coupled with a uniform hot plasma. We assumed that the bulk of the corona emission is mainly powered by the accretion disc and it is located at the transition radius (r_{tr}) where the gas pressure equates the radiation pressure in the disc. Assuming a broad line region size function of the bolometric luminosity as $R_{\text{blr}} \propto L_{\text{bol}}^{0.5}$ we have that $M_{\text{BH}} \propto \dot{M}/\dot{M}_{\text{Edd}} FWHM^4$, which leads to the final relation $L_X \propto L_{\text{UV}}^{4/7} FWHM^{4/7}$. Such a relation is remarkably consistent with the fit obtained from a sample of 550 optically selected quasars from SDSS DR7 cross matched with the XMM-*Newton* catalogue 3XMM-DR6. The toy model we presented, although simplistic, is capable of making robust predictions on the X-ray luminosities (at a given ultraviolet emission and $FWHM$) of unobscured/blue quasars, and puts observational constraints on the fraction of accretion power released in the hot plasma in the vicinity of the accretion disc, f , as a function the broad line region size, from the observed normalization of $L_X - L_{\text{UV}} - FWHM$ plane. The latter result will provide a new vantage point for the next generation of semi-analytical and magneto-hydrodynamical simulations investigating on the physical link between the accretion disc and the X-ray corona.

The proposed relation $L_X \propto L_{\text{UV}}^{4/7} FWHM^{4/7}$ does not show significant evolution with time in the redshift range covered by our data, $z = 0.3 - 2.2$, and thus it can be employed as a cosmological indicator to estimate cosmological parameters (e.g. Ω_M, Ω_Λ).

FUNDING

EL is supported by a European Union COFUND/Durham Junior Research Fellowship (under EU grant agreement no. 609412). This work has been supported by the grants PRIN-INAF 2012 and ASI INAF NuSTAR I/037/12/0.

ACKNOWLEDGMENTS

For all catalogue correlations we have used the Virtual Observatory software TOPCAT [40] available online (<http://www.star.bris.ac.uk/~mbt/topcat/>). This research has made use of data obtained from the 3XMM XMM-*Newton* serendipitous source catalogue compiled by the ten institutes of the XMM-*Newton* Survey Science Centre selected by ESA. This research made use of matplotlib, a Python library for publication quality graphics [41].

REFERENCES

- [1] Tananbaum H, Avni Y, Branduardi G, Elvis M, Fabbiano G, Feigelson E, et al. X-ray studies of quasars with the Einstein Observatory. *ApJ* **234** (1979) L9–L13. doi:10.1086/183100.
- [2] Lusso E, Risaliti G. The Tight Relation between X-Ray and Ultraviolet Luminosity of Quasars. *ApJ* **819** (2016) 154. doi:10.3847/0004-637X/819/2/154.
- [3] Vignali C, Brandt WN, Schneider DP. X-Ray Emission from Radio-Quiet Quasars in the Sloan Digital Sky Survey Early Data Release: The α_{ox} Dependence upon Ultraviolet Luminosity. *AJ* **125** (2003) 433–443. doi:10.1086/345973.

- [4] Strateva IV, Brandt WN, Schneider DP, Vanden Berk DG, Vignali C. Soft X-Ray and Ultraviolet Emission Relations in Optically Selected AGN Samples. *AJ* **130** (2005) 387–405. doi:10.1086/431247.
- [5] Steffen AT, Strateva I, Brandt WN, Alexander DM, Koekemoer AM, Lehmer BD, et al. The X-Ray-to-Optical Properties of Optically Selected Active Galaxies over Wide Luminosity and Redshift Ranges. *AJ* **131** (2006) 2826–2842. doi:10.1086/503627.
- [6] Just DW, Brandt WN, Shemmer O, Steffen AT, Schneider DP, Chartas G, et al. The X-Ray Properties of the Most Luminous Quasars from the Sloan Digital Sky Survey. *ApJ* **665** (2007) 1004–1022. doi:10.1086/519990.
- [7] Green PJ, Aldcroft TL, Richards GT, Barkhouse WA, Constantin A, Haggard D, et al. A Full Year's Chandra Exposure on Sloan Digital Sky Survey Quasars from the Chandra Multiwavelength Project. *ApJ* **690** (2009) 644–669. doi:10.1088/0004-637X/690/1/644.
- [8] Lusso E, et al. The X-ray to optical-UV luminosity ratio of X-ray selected type 1 AGN in XMM-COSMOS. *A&A* **512** (2010) A34. doi:10.1051/0004-6361/200913298.
- [9] Young M, Elvis M, Risaliti G. The X-ray Energy Dependence of the Relation Between Optical and X-ray Emission in Quasars. *ApJ* **708** (2010) 1388–1397. doi:10.1088/0004-637X/708/2/1388.
- [10] Marchese E, Della Ceca R, Caccianiga A, Severgnini P, Corral A, Fanali R. The optical-UV spectral energy distribution of the unabsorbed AGN population in the XMM-Newton Bright Serendipitous Survey. *A&A* **539** (2012) A48. doi:10.1051/0004-6361/201117562.
- [11] Jin C, Ward M, Done C. A combined optical and X-ray study of unobscured type 1 active galactic nuclei - II. Relation between X-ray emission and optical spectra. *MNRAS* **422** (2012) 3268–3284. doi:10.1111/j.1365-2966.2012.20847.x.
- [12] Suzuki N, Rubin D, Lidman C, Aldering G, Amanullah R, Barbary K, et al. The Hubble Space Telescope Cluster Supernova Survey. V. Improving the Dark-energy Constraints above $z \lesssim 1$ and Building an Early-type-hosted Supernova Sample. *ApJ* **746** (2012) 85. doi:10.1088/0004-637X/746/1/85.
- [13] Betoule M, Kessler R, Guy J, Mosher J, Hardin D, Biswas R, et al. Improved cosmological constraints from a joint analysis of the SDSS-II and SNLS supernova samples. *A&A* **568** (2014) A22. doi:10.1051/0004-6361/201423413.
- [14] Risaliti G, Lusso E. A Hubble Diagram for Quasars. *ApJ* **815** (2015) 33. doi:10.1088/0004-637X/815/1/33.
- [15] Risaliti G, Lusso E. Cosmology with AGN: can we use quasars as standard candles? *Astronomische Nachrichten* **338** (2017) 329–333. doi:10.1002/asna.201713351.
- [16] Svensson R. The pair annihilation process in relativistic plasmas. *ApJ* **258** (1982) 321–334. doi:10.1086/160081.
- [17] Svensson R. Steady mildly relativistic thermal plasmas - Processes and properties. *MNRAS* **209** (1984) 175–208. doi:10.1093/mnras/209.2.175.
- [18] Zdziarski AA, Ghisellini G, George IM, Fabian AC, Svensson R, Done C. Electron-positron pairs, Compton reflection, and the X-ray spectra of active galactic nuclei. *ApJ* **363** (1990) L1–L4. doi:10.1086/185851.
- [19] Haardt F, Maraschi L. A two-phase model for the X-ray emission from Seyfert galaxies. *ApJ* **380** (1991) L51–L54. doi:10.1086/186171.
- [20] Haardt F, Maraschi L. X-ray spectra from two-phase accretion disks. *ApJ* **413** (1993) 507–517. doi:10.1086/173020.
- [21] Svensson R, Zdziarski AA. Black hole accretion disks with coronae. *ApJ* **436** (1994) 599–606. doi:10.1086/174934.

- [22] Di Matteo T. Magnetic reconnection: flares and coronal heating in active galactic nuclei. *MNRAS* **299** (1998) L15–L20. doi:10.1046/j.1365-8711.1998.01950.x.
- [23] Róžańska A, Czerny B. Vertical structure of the accreting two-temperature corona and the transition to an ADAF. *A&A* **360** (2000) 1170–1186.
- [24] Haardt F, Maraschi L, Ghisellini G. A model for the X-ray and ultraviolet emission from Seyfert galaxies and galactic black holes. *ApJ* **432** (1994) L95–L99. doi:10.1086/187520.
- [25] Galeev AA, Rosner R, Vaiana GS. Structured coronae of accretion disks. *ApJ* **229** (1979) 318–326. doi:10.1086/156957.
- [26] Merloni A, Fabian AC. Coronal outflow dominated accretion discs: a new possibility for low-luminosity black holes? *MNRAS* **332** (2002) 165–175. doi:10.1046/j.1365-8711.2002.05288.x.
- [27] Liu BF, Mineshige S, Shibata K. A Simple Model for a Magnetic Reconnection-heated Corona. *ApJ* **572** (2002) L173–L176. doi:10.1086/341877.
- [28] Balbus SA. Enhanced Angular Momentum Transport in Accretion Disks. *ARAA* **41** (2003) 555–597. doi:10.1146/annurev.astro.41.081401.155207.
- [29] Lusso E, Risaliti G. Quasars as standard candles. I. The physical relation between disc and coronal emission. *A&A* **602** (2017) A79. doi:10.1051/0004-6361/201630079.
- [30] Shen Y, Richards GT, Strauss MA, Hall PB, Schneider DP, Snedden S, et al. A Catalog of Quasar Properties from Sloan Digital Sky Survey Data Release 7. *ApJS* **194** (2011) 45. doi:10.1088/0067-0049/194/2/45.
- [31] Rosen SR, Webb NA, Watson MG, Ballet J, Barret D, Braito V, et al. The XMM-Newton serendipitous survey. VII. The third XMM-Newton serendipitous source catalogue. *A&A* **590** (2016) A1. doi:10.1051/0004-6361/201526416.
- [32] Foreman-Mackey D, Hogg DW, Lang D, Goodman J. emcee: The MCMC Hammer. *PASP* **125** (2013) 306–312. doi:10.1086/670067.
- [33] Trippe S. AGN Broad Line Regions Scale with Bolometric Luminosity. *Journal of Korean Astronomical Society* **48** (2015) 203–206. doi:10.5303/JKAS.2015.48.3.203.
- [34] Kaspi S, Maoz D, Netzer H, Peterson BM, Vestergaard M, Jannuzi BT. The Relationship between Luminosity and Broad-Line Region Size in Active Galactic Nuclei. *ApJ* **629** (2005) 61–71. doi:10.1086/431275.
- [35] King AR, Pringle JE, Livio M. Accretion disc viscosity: how big is alpha? *MNRAS* **376** (2007) 1740–1746. doi:10.1111/j.1365-2966.2007.11556.x.
- [36] Jiang YF, Stone JM, Davis SW. A Global Three-dimensional Radiation Magneto-hydrodynamic Simulation of Super-Eddington Accretion Disks. *ApJ* **796** (2014) 106. doi:10.1088/0004-637X/796/2/106.
- [37] Cao X. An accretion disc-corona model for X-ray spectra of active galactic nuclei. *MNRAS* **394** (2009) 207–213. doi:10.1111/j.1365-2966.2008.14347.x.
- [38] Liu JY, Qiao EL, Liu BF. Revisiting the Structure and Spectrum of the Magnetic-reconnection-heated Corona in Luminous AGNs. *ApJ* **833** (2016) 35. doi:10.3847/1538-4357/833/1/35.
- [39] Czerny B, Li YR, Hryniewicz K, Panda S, Wildy C, Sniegowska M, et al. Failed Radiatively Accelerated Dusty Outflow Model of the Broad Line Region in Active Galactic Nuclei. I. Analytical Solution. *ApJ* **846** (2017) 154. doi:10.3847/1538-4357/aa8810.
- [40] Taylor MB. TOPCAT & STIL: Starlink Table/VOTable Processing Software. Shopbell P, Britton M, Ebert R, editors, *Astronomical Data Analysis Software and Systems XIV* (2005), *Astronomical Society of the Pacific Conference Series*, vol. 347, 29.

- [41] Hunter JD. Matplotlib: A 2D Graphics Environment. *Computing in Science and Engineering* **9** (2007) 90–95. doi:10.1109/MCSE.2007.55.